

Investigating and understanding diffraction patterns using Fourier analysis with variations of the 4f Optical System

Jacky Cao, Fourier Optics, Friday, Lab Partner: Thomas Spriggs

Dates of experiment: 10/02/2017 to 17/03/2017, Date of report: 19/03/2017

Through the study of the Fourier transforms it is possible to understand diffraction patterns. The volume flow rate of a fluid can be expressed functionally as derived by Poiseuille and Hagen. This relationship can be rearranged so that the viscosity of water can be experimentally determined. Using a capillary tube and altering the height of water in a tank, the volume and mass of water which has flowed out in a time period can be measured. Using this data, it is then possible to calculate a value for the viscosity of water. The average value was determined to be 1.00 ± 0.03 mPa s, which does not agree with the literature value, 1.679 mPa s.

I. INTRODUCTION

In the field of optics, a diffraction pattern can be produced when a coherent beam of radiation falls onto a partially opaque object [1]. The pattern can then be viewed at a “far-field” distance, this length being larger than the initial size of the object, allowing for the spreading of light due to diffraction to dominate in the observation plane [2].

The usage of diffraction patterns includes the studying of crystalline structures. Through X-ray and electron diffraction it is possible to obtain accurate information about the identity of phases present, atomic ordering, and for recognising different metallurgical constituents within a specimen. This allows for potential applications within the pharmaceutical industry for example, where early analysis of different mixtures and compounds can be cost and time saving. [3, 4]

Another application could potentially involve using the diffraction pattern within an illumination system so that x-ray phase contrast microscopy and interferometry can be performed [5]. This could be used to enhance the visibility of fine scale structures, this being especially useful in biology as quantitative information can be obtained about a sample from just phase-contrast images [6].

With these varying applications we find that in order to fully understand diffraction patterns and how they form, we must look at the mathematics behind them.

The main mathematical tool that we must use in building our understanding is Fourier analysis, more specifically, Fourier transforms. A Fourier transform is a way to represent a function in terms of a superposition of sinusoidal functions, with the explicit conditions of the function being defined over an infinite interval and having no particular periodicity [1].

The following theory/mathematics has been adapted from Optics f2f [2].

The Fourier transform $F(u)$ of a single function $f(x)$ can be stated as,

$$F(u) = \mathcal{F}[f(x)](u) = \int_{-\infty}^{\infty} f(x)e^{-i2\pi ux}dx, \quad (1)$$

where (u) is the dependent Fourier variable. This expression tells us the spectrum of frequencies required to form the function $f(x)$.

We can also operate on the initial function then Fourier transform it. In Table I we find the group of functions known as the Fourier transform properties.

The convolution property can be better understood as follows - if we convolve two functions of x , $g(x)$ and $h(x)$,

Property	\mathbf{f}	\mathbf{F}
Linearity	$g(x) + h(x)$	$G(u) + H(u)$
Translation	$f(x-a)$	$F(u)e^{-i2\pi ua}$
Scaling	$f(x/a)$	$aF(ua)$
Convolution	$(g * h)(x)$	GH
Inverse Convolution	gh	$(G * H)(u)$

TABLE I: The Fourier transform properties - different functions \mathbf{f} and their output \mathbf{F} when they have been Fourier transformed using equation 1.

then that is defined as,

$$(g * h)(x) = \int_{-\infty}^{\infty} g(x')h(x-x')dx'. \quad (2)$$

In words, a convolution can be stated as *sliding one function through the other and summing the area which overlaps*. This can be especially useful if we are translating a function and making multiple copies of it.

In the application of optics, the Fourier variable that has been repeatedly used is called the spatial frequency, u . It is defined as the *number of waves per unit length*, and is the real space analogue of frequency. Its mathematical form for the far-field case can be written as a mapping between the Fourier variable and real space position,

$$u = \frac{x}{\lambda z}, \quad (3)$$

where x is the position in real space, λ is the wavelength of radiation being used to illuminate the object, and z is the distance ‘downstream’ from the object.

When considering diffraction gratings, we can describe the physical makeup of one using a mathematical function. This function could then be manipulated using the different Fourier transform properties as found in Table I. The result of which is an expression which can describe the diffraction pattern observed.

When working with optics we must make the distinction between *real* and *Fourier* space. The former indicating the plane in which a diffraction grating would sit, and the latter representing the plane when the diffraction grating (or any radiation) has been Fourier transformed.

There are some basic shapes which can be used as the object which is being illuminated by radiation: a rectangular slit, and a circular aperture. However to consider these cases we must move into 2 dimensions and consider a 2D Fourier transform.

A 2D Fourier transform has the form of a double integral, so equation 1 becomes,

$$F(u, v) = \int_{-\infty}^{\infty} \int_{-\infty}^{\infty} f(x, y) e^{-i2\pi(ux+vy)} dx dy, \quad (4)$$

where u and v are the spatial frequencies corresponding to the x and y directions respectively.

The mathematics can still be used as a tool, but now an extra set of terms must be considered.

In Table II we find the functional form of the shapes and their output when they are Fourier transformed, the derivations can be found on pp. 63-64 of *Optics f2f* [2].

Shape	f	F
Rectangle	$\text{rect}(x/a)$	$a \text{sinc}(\pi ua)$
Circle	$\text{circ}(\rho/D)$	$(\pi D^2/4) \text{jinc}(\pi \varpi D)$

TABLE II: Function of each specified shape and it's Fourier transform. Where a is the width of a rectangular pulse, $\rho = \sqrt{x^2 + y^2}$ is the radial distance, $\varpi = \sqrt{u^2 + v^2}$ is the Fourier equivalent of this, and D is the diameter of the circle.

With the one dimensional rect function, the Fourier function is a *sinc*, this can be defined in the more familiar terms of $\text{sinc}(\pi ua) = \sin(\pi ua)/(\pi ua)$. Similarly, the result for the circ is a *jinc* function, which is a Bessel function of the first order. So rewritten it is: $\text{jinc}(\pi \varpi D) = J_1(\pi \varpi D)/(\pi \varpi D)$.

To repeat one of these functions one can use a *comb* function - a sum of regularly spaced δ -functions. In the context of optics, the real space δ -function contains all spatial frequencies with an equal amplitude. We can Fourier transform the δ -function so $\mathcal{F}[\delta(x)](u) = 1$.

Defining the comb function as a mathematical expression is thus,

$$\text{comb}_N\left(\frac{x}{d}\right) = \sum_{n=-\frac{(N-1)}{2}}^{\frac{(N-1)}{2}} \delta(x - nd), \quad (5)$$

where the variable x has been scaled by the value of d , and N is the number of δ -functions.

If we were to Fourier transform this finite comb, then the outcome is a discrete sum of phasors,

$$\begin{aligned} \mathcal{F}\left[\text{comb}_N\left(\frac{x}{d}\right)\right](u) &= e^{-i(N-1)\pi ud} + e^{-i(N-1)\pi ud} e^{i2\pi ud} \\ &\quad + \dots + e^{i(N-1)\pi ud}. \end{aligned} \quad (6)$$

This is particularly useful in optics when the diffraction gratings can expand from being a single aperture to many apertures e.g. a single slit versus a coarse grating of many slits.

We can relate the mathematics to experimentation through shining radiation through a diffraction grating then observing the diffraction pattern at some distance later.

What is observed can be quantified in terms of the *intensity*, this is found by taking the absolute value of the Fourier transform, squaring it, and applying a scaling factor $I_0/(\lambda^2 z^2)$ - where I_0 is a number, λ is the wavelength of radiation, and z is the distance 'downstream'.

Using an optical system which composes of a laser and two identical lenses, the radiation of the laser passing through a diffraction grating can be focused to distances

equal to multiples of the focal length of the lenses. The resulting pattern can then be observed on a screen or with a CCD. The setup in mind is called the *4f* optical system - where each component is a focal length, f , apart.

The laser and the lenses have their own mathematical descriptions attached to them.

The profile of the laser beam is of a *gaussian* shape, the mathematical definition and Fourier transform of which can be found in *Optics f2f*. The lenses act as a magnifier, this results in the diffraction pattern shifting from being at a far-field distance z , to the focal length distance f of the lens.

Using variations of the *4f* system we can explore and study different diffraction patterns and attempt to relate them back to their mathematics.

II. METHOD

To create and observe diffraction patterns we needed to set-up the *4f* system. Figure 1 shows this experimental setup.

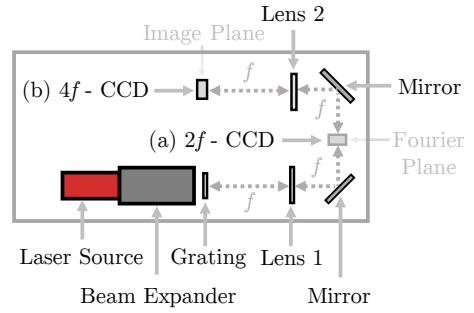


FIG. 1: A plan view schematic of the experimental set-up used to collect data. f are the focal lengths of lenses 1 and 2. Each component was attached to an optical breadboard. (a) *2f* optical system used in studying the Fourier plane (b) *4f* optical system used in studying the image plane.

A coherent laser source of wavelength ~ 635 nm was used as our source of radiation. A $\times 10$ beam expander was placed directly after this to allow the beam width to be adjusted during experimentation, this was done in an attempt to focus the majority of the light onto area of the diffraction grating.

To place the lenses at the correct f distances their focal lengths had to be measured. This was done by placing each lens at the beam expander, a screen was then moved closer and further away from the source until the brightest and sharpest spot could be observed. At that distance was thus the focal length, measured with a metre ruler we found that for both lens 1 and 2, their focal lengths were 48 ± 1 cm.

Due to the constraint with the size of the breadboard, mirrors were used to reflect the light so that the set-up would take up less space. Two were positioned so that light could be reflected into a CCD camera, and ensuring that the focal length distances were preserved.

The camera was moved at various stages of experimentation, from being in the Fourier plane at a distance of $2f$ to a distance of $4f$ when we wanted observations made within the image plane.

Our CCD was controlled using the manufacturer's software, images were saved and then later analysed using modules compiled in Python and in MATLAB.

They would convert the image from RGB colour into grayscale, calculate intensity profiles for the x and y directions of the image, and then an attempt at model fitting would be made.

The grayscale images were obtained by converting the three RGB values from a pixel into a singular value defined as the CIE 1931 Linear Luminance,

$$Y_{\text{linear}} = 0.2126R + 0.7152G + 0.0722B, \quad (7)$$

where R, G, B are the respective *red*, *green*, and *blue* values from the pixel [7]. The possible value range for a pixel was fixed between 0 (total black) to 255 (total white).

The intensity profiles were created by locating the rows (and columns) within the images that contained the greatest amount of pixels with the value of 255, those were then averaged together.

A graph could then be plotted, and subsequently a χ^2 value could be calculated when a theoretical model was compared to the intensity graphs.

Throughout our research we varied the gratings that were used, they were placed within a holder just after the beam expander and the pattern that they created was observed at different distances.

Adjustments had to be made so that the pattern observed was as clear as possible. A recurring problem was the over-saturation of the diffraction pattern. This was corrected for by using a neutral density filter and adjusting the exposure time and the gain of the CCD within the software.

To measure small scale distances of features on the diffraction grating, a travelling microscope with a Vernier scale was used.

III. RESULTS

Figure 2 show multiple plots of the horizontal intensity against the distance along the x direction for different diffraction patterns in the Fourier plane.

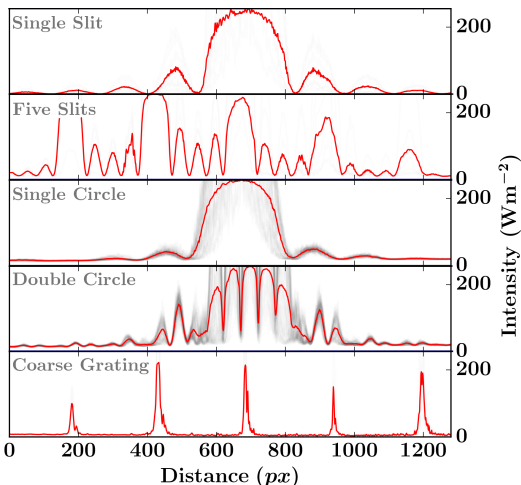


FIG. 2: The horizontal intensity profiles of diffraction patterns within the Fourier plane created with different diffraction gratings. The shadow behind the diagrams are the rows that were averaged to create the profile that is shown.

Figures 3(a), 3(b), and 3(c) show the horizontal intensity data for the single slit, five slits, and double circle slit plotted with a theoretical model. The reduced χ^2 values have been calculated and can be found in Table III.

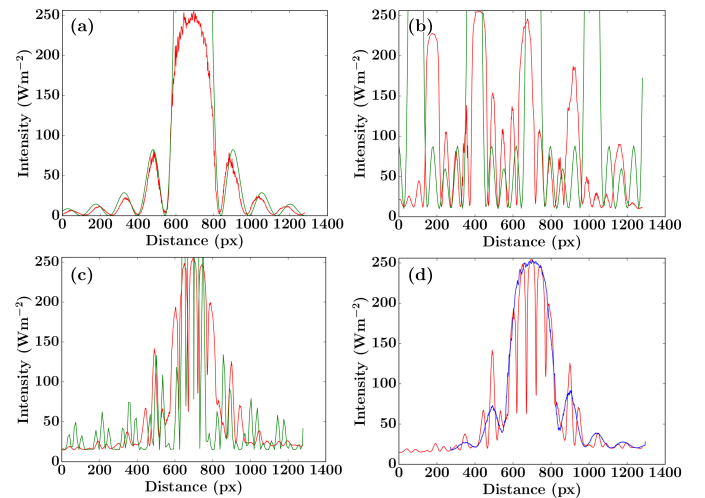


FIG. 3: Theoretical model (green), horizontal intensity data (red), and vertical intensity data (blue) - data from Fourier plane. The uncertainties for the horizontal and vertical intensities are too small to be seen. (a) Single slit with model. (b) Five slits with model. (c) Double circles with model. (d) Envelope nature of double circle slit.

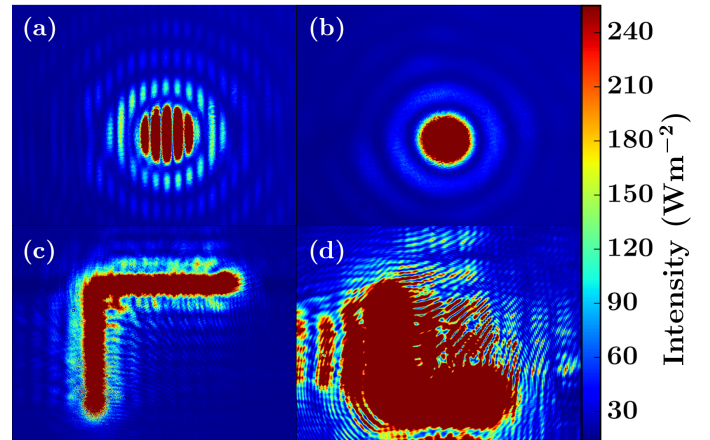


FIG. 4: Intensity maps of four different diffraction patterns taken from different planes: (a) double circle grating in Fourier plane, (b) single circle grating in Fourier plane, (c) L grating in image plane, (d) L grating in '3f' plane.

The horizontal and vertical intensity graphs for the double circular slit have been superimposed and can be found in Figure 3(d).

Table IV shows the slit widths of three different coarse gratings as measured in real space, and calculated from Fourier space.

Grating	χ^2
Single Slit	36.8
Five Slits	8.24×10^6
Double Circle	6.55×10^4

TABLE III: A theoretical model was applied to the single slit, five slits, and double circle diffraction gratings. Only the single slit provided a fit that would allow us to calculate a χ^2 value.

IV. DISCUSSION

From just an initial inspection of Figure 2 we can discern the possible mathematics involved with the diffrac-

Grating	Real Space [mm]	Fourier Space [mm]
1	0.20 ± 0.05	0.11 ± 0.03
2	0.12 ± 0.05	0.11 ± 0.01
3	0.08 ± 0.05	0.05 ± 0.01

TABLE IV: For each coarse diffraction grating, the diffraction grating slit width is shown as measured in real space, and as calculated in Fourier space.

tion patterns.

We can see the application of the convolution theorem within the functions for the five slits and the double circle grating. Respectively, it is a rect convolved with comb_5 , and a circ convolved with comb_2 .

Looking at the calculated χ^2_ν values for these two gratings we see that they are not near unity at all, in fact they are orders of magnitude out. The basic requirement for the theoretical models to be a good fit to the data is that they be close to the value of 1 [8]. For the single slit we see that the model used provides a closer fit than the others do, but it is still not a good.

While we do understand the functions of the gratings and conversely their Fourier transforms, there is much difficulty in implementing this within a program. The trouble mainly arises in attempting to scale and translate the model to fit the data.

The images that we collected are not perfect, we can see that with the intensity profile for the five slits. The principal maximas should all be the same height, as well as the first and last subsidiary maximas. This inevitably leads to a difficult fit with the model. We understood that this arose from the laser beam not creating an even illumination, the top half having less light.

We can further understand the double circle slit, the pattern of the convolved circ function retains its original Airy disk profile but it now also contains cosine-squared interference fringes (Figures 4(a) and 4(b)). If this is superimposed with a jinc^2 function, one can fit into the other - an envelope, as can be seen in Figure 3(d). This is similar to the sinc^2 enveloping of Young's double slit experiment [2].

In trying to develop our knowledge of real and Fourier space, we attempted to measure the slit width of a slit of three different coarse gratings in real space and from Fourier space. Our results are shown in Table IV, we see that while the measurements from real space agree with their Fourier counterpart within their experimental error, the converse is not true.

We suspect this could be due to how we defined the size of a pixel in Fourier space, our calculations for the first and third gratings were based off how we calculated what one pixel equals in Fourier space ($\sim 36.9\text{m}$). If this was incorrect, which we assume it was, then our other

values are incorrect too.

After exploring patterns within the Fourier plane, we then moved into the image plane. In Figure 4(c) the pattern is a rotated L shape, the original L grating was the correct way up. We find that there has been a parity change from (x, y) to $(-x, -y)$. This occurs when we take the Fourier transform of the field in the Fourier plane, it is an inverse transform [2].

A curious expansion to our research can be seen in Figure 4(d). The L grating diffraction pattern as seen in a '3f' system, to create this we moved the source and grating to be directly behind the first lens. This pattern has features from both the Fourier and image plane. In the centre there is a clear L, something which can be found in the image plane, and to the sides we can see what appears to be sinc^2 pattern features. While the mathematics is beyond our scope, we could suggest that this pattern was formed by applying a convolution to the initial function as it has features from both planes.

Improvements could be made to our investigation to improve the quality of data taken. For example working harder to reduce saturation, during experimentation we had not fully considered the possible effects bias might have on the images that were taking. With future experimentation we would reduce things such as CCD bias by pre-taking images of the dark room so that any stray pixels could be removed during analysis.

Other improvements could be made such as collecting multiple repeats of the diffraction pattern images with different CCD cameras. These images could then be averaged together and a possible uncertainty could be calculated for them.

In experimentation we did omit the fact that?

V. CONCLUSIONS

In conclusion it has been possible to investigate and understand different diffraction patterns, through producing them within a $4f$ system, and then through comparing the intensity graphs with theoretical models.

Lorem ipsum dolor sit amet, consectetur adipiscing elit. Etiam lobortis facilisis sem. Nullam nec mi et neque pharetra sollicitudin. Praesent imperdiet mi nec ante. Donec ullamcorper, felis non sodales commodo, lectus velit ultrices augue, a dignissim nibh lectus placerat pede. Vivamus nunc nunc, molestie ut, ultricies vel, semper in, velit. Ut porttitor. Praesent in sapien. Lorem ipsum dolor sit amet, consectetur adipiscing elit. Duis fringilla tristique neque. Sed interdum libero ut metus. Pellentesque placerat. Nam rutrum augue a leo. Morbi sed elit sit amet ante lobortis sollicitudin. Praesent blandit blandit mauris. Praesent lectus tellus, aliquet aliquam, luctus a, egestas a, turpis. Mauris lacinia lorem sit amet ipsum. Nunc quis urna dictum turpis accumsan semper.

-
- [1] K. F. Riley, M. P. Hobson, and S. J. Bence. *Mathematical Methods for Physics and Engineering*. Cambridge University Press, Cambridge, UK, 2010.
- [2] C. S. Adams and I. G. Hughes. *Optics f2f, from Fourier to Fresnel*. Clarendon Press, Oxford, UK, 2017.
- [3] K. W. Andrews, D. J. Dyson, and S. R. Keown. *Interpretation of Electron Diffraction Patterns*. Hilger & Watts Ltd, London, UK, 1967.
- [4] J. P. Smit, R. B. McClurg. *X-ray Powder Diffraction Pattern Indexing for Pharmaceutical Applications*. Pharmaceutical Technology, January 2013, Vol. 37, No. 1.
- [5] A. R. Lang, et al. *Single-slit diffraction patterns of sub-nanometre-wavelength synchrotron radiation*. Journal of Physics D: Applied Physics, 1987, Vol. 20, No. 4, pp. 541-544.
- [6] S. C. Mayo, et al. *X-ray phase-contrast microscopy and microtomography*. Optical Express, 2003, Vol. 11, No. 19, pp. 2289-2302.

- [7] M. Stokes, et al. *A Standard Default Color Space for the Internet*. November 1996, available at: <https://www.w3.org/Graphics/Color/sRGB>, accessed: 11th February 2017.
- [8] I. G. Hughes and T. P. A. Hase. *Measurements and their Uncertainties*. Oxford University Press, Oxford, UK, 2010.

Appendix

Appendix